Acta Cryst. (1977). A33, 301–307

The (Q, ω) Transmission Function of a Crystal–Chopper Neutron Spectrometer*

BY G. QUITTNER

Österreichische Studiengesellschaft für Atomenergie GmbH, Lenaugasse 10, *A*-1082 *Wien, Austria*

(*Received* 9 *October* 1975; *accepted* 21 *September* 1976)

A model of a crystal–chopper neutron spectrometer comprising the interrelated reciprocal-space, direct-space and time effects is presented. In this model the transmission function of a particular time-analyser channel is calculated containing information both on resolution and counting rate. The problems of numerical accuracy arising in the application of the formulae are briefly discussed.

1. Introduction

The importance of calculating the transmission function of thermal neutron spectrometers for the design and interpretation of scattering experiments has been widely recognized and has resulted in a considerable number of publications describing such calculations. While the number of papers on triple-axis, pure-chopper and rotating-crystal spectrometers is considerable, publications on the hybrid, *i.e.* a crystal–chopper spectrometer, are scanty.

There is one detailed paper by Steinsvoll (1973) where the Nielsen–Bjerrum-Møller (1969) method of independent resolution vectors is used. Another calculation concerning the same instrument by Samuelsen (1971) replaces the triple-axis-spectrometer (TAS) acceptance function by a function simulating the chopper action and uses, after this replacement, the Cooper & Nathans (1967) TAS formulae. In this instrument the chopper is placed after the sample.

A third calculation is mentioned in a paper by Kleb, Ostrowski, Price & Rowe (1973) and is said to have been done along the lines of Cooper & Nathans (1967) but no details are given. In this instrument as well as in the one we are interested in [D-7 of the Laue–Langevin Institute in Grenoble; for a description see Bauer, Seitz & Just (1975)] the chopper is placed before the sample.

The principle of quadratic superposition of widths has been widely used, especially in conjunction with time-of-flight spectrometers, from the early days up to the present: it consists in calculating separately the uncertainties due to defining elements and/or 'smearing' processes and adding them quadratically to obtain the final width. In most applications of this principle the addition of the squared widths is done along the time-of-flight axis. Nielsen & Bjerrum-Møller (1969) have generalized this principle to apply to directions in $(\mathbf{Q}, \omega)$ space.

In view of the strong correlations between reciprocal-space, time and direct-space effects in the hybrid spectrometer we thought that an independent calculation by more traditional methods – similar to that of Cooper & Nathans (1967) for TAS and Komura & Cooper (1970) for the double-chopper spectrometer – which do not presuppose the 'incoherent' superposition of widths, might be useful. Moreover, the present calculation considers not only resolution effects (as given by a normalized resolution function), but also the counting rate (therefore the name 'transmission function'), a feature absent in previous hybrid-spectrometer calculations.

The essential points of such a calculation are outlined in § 2. In § 3 a model of the hybrid spectrometer comprising reciprocal-space, time and direct-space effects is presented and the corresponding transmission function calculated. In § 4 a numerical example is given and some problems of numerical accuracy arising in applying the formulae are pointed to.

Glossary of symbols used in the text

Bold-face letters stand for vectors (*e.g.* $\mathbf{k}_{0M}$), italic letters for scalar quantities (*e.g.* k_{0M}). Also, if X is a general value of a quantity, then X_0 is its central (or nominal) value, and δX its deviation from the latter, *i.e.* $X = X_0 + \delta X$.

$\mathbf{Q}$	wavenumber transfer in the scattering
ω	energy transfer in the scattering
$\hbar$	Planck' constant, divided by 2π
m	neutron mass
$\mathbf{k}_M$	wavenumber of the incoming neutron
$\mathbf{k}_A$	wavenumber of the outgoing neutron
q_x	component of $\mathbf{Q}-\mathbf{Q}_0$ in the direction of $\mathbf{Q}_0$
q_y	component of $\mathbf{Q}-\mathbf{Q}_0$ perpendicular to $\mathbf{Q}_0$
M	projection of $\mathbf{k}_M$ onto $\mathbf{Q}$
A	projection of $\mathbf{k}_A$ onto $\mathbf{Q}$
α	angle $(\mathbf{Q}, \mathbf{Q}_0)$
τ	nominal time of flight
$\Delta\tau$	channel width
$\mathscr{F}(Q, \omega, \tau)$	transmission function density
l	'height' of the general scattering triangle, *i.e.* the length of the projection of $\mathbf{k}_M$ or $\mathbf{k}_A$ perpendicular to $\mathbf{Q}$
L_1	length of the primary flight path

* Work supported in part by Fonds zu Förderung der wissenschaftlichen Forschung in Österreich.

L_2 length of the secondary flight path
$\mathbf{e}_{0A}$ unit vector in the direction of $\mathbf{k}_{0A}$
ϱ angle $(\mathbf{k}_{0M},\mathbf{Q}_0)$
λ angle $(\mathbf{k}_{0A},\mathbf{Q}_0)$
θ Bragg angle at the monochromator crystal
α_1 primary collimation of the monochromator
γ_M angle $(\mathbf{k}_M,\mathbf{k}_{0M})$
γ_A angle $(\mathbf{k}_A,\mathbf{k}_{0A})$
β_M mosaic width of the monochromator crystal
U space coordinate perpendicular to the central incoming beam, at the chopper
v_{Ch} circumferential speed of the chopper slit
ΔCh width of the chopper slit, both the rotating and the stationary
δt $=t-\tau$
x,y space coordinates at the sample
Δr width of the cylindrical sample
φ scattering angle = angle $(\mathbf{k}_{0M},\mathbf{k}_{0A})$
V space coordinate perpendicular to the central outgoing beam, at the detector position
T overall neutron transmission function
$T_1 \ldots T_7$ transmission functions of the defining elements 1 ... 7
B_{ij} coefficients of $q_x,q_y\delta\omega,t,x,y$ in the exponents of $T_1 \ldots T_7$
W_l pre-exponential factor resulting from the integration over l
DC duty cycle of the chopper
$P_M(k_{0M})$ top reflectivity of the monochromator crystal
$\epsilon(k_{0A})$ detector efficiency
$V(q_z)$ vertical resolution function
$\sqrt{\pi/W_t}$ pre-exponential factor resulting from vertical integration
$\alpha_{1V},\beta_{MV},\alpha_{2V}$ vertical collimations and vertical mosaic corresponding to the horizontal $\alpha_1,\beta_M,\alpha_2$
α_{3V} vertical collimation sample-detector
$\sqrt{\pi/W_x},\sqrt{\pi/W_y}$ pre-exponential factors resulting from the integration over the coordinates x,y at the sample
$\mathscr{A}_{xx},\mathscr{A}_{xy}$ *etc.* resolution coefficients
C.R. counting rate
$\phi_0(k_{0M})$ k-density of neutron flux density of the source
$S(\mathbf{Q},\omega)$ van Hove scattering function of the sample

2. Principles of transmission function calculations in hybrid spectrometers

The nature and the methods of calculation of the TAS transmission function have been well understood since the Cooper–Nathans (1967) paper and a number of subsequent papers. Therefore we will keep as close as possible to these methods, modifying them only where necessary.

The TAS transmission function is defined over $\mathbf{Q}$ and ω, *i.e.* over reciprocal-space variables, and only such variables occur in the usual calculations. One considers, in essence, the manifold of all wavenumber vector pairs $(\mathbf{k}_M,\mathbf{k}_A)$ of incoming and outgoing neutrons resulting in a given wavenumber transfer $\mathbf{Q}$ and energy transfer ω. This manifold is shown in Fig. 1.

$$M=\tfrac{1}{2}\left[(Q_0+q_x)+\frac{\omega_0+\delta\omega}{\frac{\hbar}{2m}(Q_0+q_x)}\right] \tag{1}$$

$$A=\tfrac{1}{2}\left[(Q_0+q_x)-\frac{\omega_0+\delta\omega}{\frac{\hbar}{2m}(Q_0+q_x)}\right] \tag{2}$$

are the projections of the $\mathbf{k}_M$ and $\mathbf{k}_A$ vectors onto $\mathbf{Q}$ and

$$\alpha=\arctan\frac{q_y}{Q_0+q_x} \tag{3}$$

is the angle between the $\mathbf{Q}$ considered and the reference $\mathbf{Q}_0$ [see also equations (16)–(18) of Quittner, 1971].

A difference of the hybrid spectrometer as against the TAS is that time must be connected with the reciprocal-space variables. This is done through the time-of-flight equation

$$\frac{\hbar}{m}t=\frac{L_1}{k_M}+\frac{L_2}{k_A} \tag{4}$$

at several places in the calculations.

Instead of a transmission function $\mathscr{T}(\mathbf{Q},\omega)$ one has to calculate a time-of-flight density of transmission function $\mathscr{T}(\mathbf{Q},\omega,\tau)$, such that its integral over the channel width $\Delta\tau$ gives an ordinary transmission function. When a Cooper–Nathans type result is aimed at – a resolution ellipsoid in $(\mathbf{Q},\omega)$ space centred on a point $(\mathbf{Q}_0,\omega_0)$ of its maximum – the centre or supporting point must be calculated as

$$k_{0A}(\tau)=\frac{L_{20}}{\frac{\hbar}{m}\tau-\frac{L_{10}}{k_{0M}}} \tag{5}$$

$$\mathbf{k}_{0A}(\tau)=\mathbf{e}_{0A}\,.\,k_{0A}(\tau) \tag{6}$$

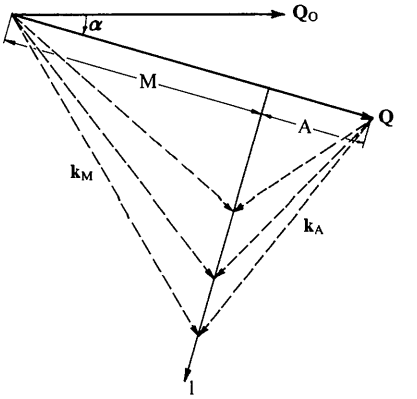

Fig. 1. The manifold of vector pairs $(\mathbf{k}_{0M},\mathbf{k}_{0A})$ resulting in the same wavenumber transfer $\mathbf{Q}$ and energy transfer ω. $\mathbf{Q}_0$ is the nominal wavenumber transfer. α, M, A are functions of $\mathbf{Q}$, ω given by equations (1–3); l, the height of the scattering triangle, is the parameter of this manifold.

where $\mathbf{e}_{0A}$ is a unit vector in the direction of the central secondary flight path,

$$\mathbf{Q}_0(\tau)=\mathbf{k}_{0M}-\mathbf{k}_{0A}(\tau) \tag{7}$$

$$\omega_0(\tau)=\frac{\hbar}{2m}[k_{0M}^2-k_{0A}^2(\tau)]. \tag{8}$$

The two angles ϱ and λ determining, for each τ, the nominal scattering triangle, are

$$\varrho(\tau)=\angle(\mathbf{Q}_0(\tau),\mathbf{k}_{0M}) \tag{9}$$

$$\lambda(\tau)=\angle(\mathbf{Q}_0(\tau),\mathbf{k}_{0A}(\tau)). \tag{10}$$

3. A model of hybrid spectrometer and calculation of its transmission function

The model (Fig. 2) comprises what is thought to be a minimum of features to account for the essential reciprocal-space, time and direct-space effects: more complicated models are of course possible. The essential calculations are confined to two-dimensional Q's, the inclusion of the q_z dimension being done in complete analogy with the TAS case (see Quittner, 1971, 1972). There is a primary collimation with a transmission

$$T_1=\exp\left[-\left(\frac{-\frac{2\delta k_M\tan\theta}{k_{0M}}+\gamma_M}{\alpha_1}\right)^2\right]; \tag{11}$$

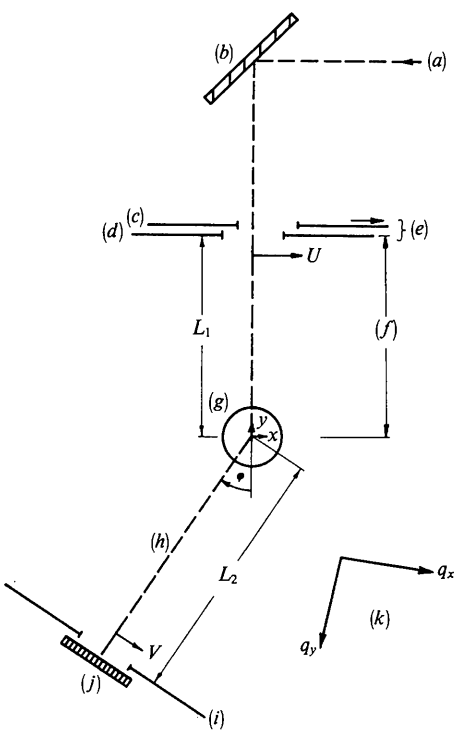

Fig. 2. Model of hybrid spectrometer consisting of a crystal, a disc chopper (a moving and a stationary diaphragm) and a cylindrical sample: (*a*) neutron source; (*b*) crystal; (*c*) moving diaphragm; (*d*) stationary diaphragm; (*e*) disc chopper; (*f*) primary flight path; (*g*) sample; (*h*) secondary flight path; (*i*) detector diaphragm; (*j*) detector; (*k*) orientation of q_x and q_y.

a crystal with

$$T_2=\exp\left[-\left(\frac{-\frac{\delta k_M\tan\theta}{k_{0M}}+\gamma_M}{\beta_M}\right)^2\right]; \tag{12}$$

and a rotating chopper disc with

$$T_3=\exp\left[-\left(\frac{U-v_{\mathrm{Ch}}\,.\,\delta t}{\Delta\mathrm{Ch}}\right)^2\right]; \tag{13}$$

where v_{Ch} is the circumferential speed of the chopper slit, and U a space coordinate perpendicular to the direction of the incoming beam; a stationary diaphragm with

$$T_4=\exp-\left(\frac{U}{\Delta\mathrm{Ch}}\right)^2; \tag{14}$$

a cylindrical sample with the normalized density distributions

$$T_5=\frac{1}{\sqrt{\pi}\Delta r}\exp\left[-\left(\frac{x}{\Delta r}\right)^2\right] \tag{15}$$

$$T_6=\frac{1}{\sqrt{\pi}\Delta r}\exp\left[-\left(\frac{y}{\Delta r}\right)^2\right]; \tag{16}$$

and a diaphragm before the detector with

$$T_7=\exp\left[-\left(\frac{V}{\Delta V}\right)^2\right]. \tag{17}$$

The elementary scattering event is: a primary neutron with its wavenumber vector $k_{0M}+\delta k_M$ and a direction γ_M starts at U at a time δt, is scattered at x,y, travels therefrom, with a wavevector of magnitude $k_{0A}+\delta k_A$ and direction γ_A, towards the detector and arrives there at V.

The overall transmission

$$T=T_1\,.\,T_2\,.\,T_3\,.\,T_4\,.\,T_5\,.\,T_6\,.\,T_7 \tag{18}$$

depends, as it stands, on δk_M, δk_A, γ_M, γ_A, U, V, δt, x, y. Many of these are interdependent. One can choose the arguments $q_x,q_y,\delta\omega$ of the transmission function and any three of the variables listed above as independent – we decide on $\delta t,x,y$ – and eliminate the remaining ones: δk_M, δk_A, γ_M, γ_A, U, V by the following relations:

$$\delta L_1=-y;\quad \delta L_2=x\sin\varphi+y\cos\varphi \tag{19}$$

$$k_{0M}\delta k_M-k_{0A}\delta k_A=M_0\delta M-A_0\delta A \tag{20}$$

$$\frac{\hbar}{m}\delta t=\frac{\delta L_1}{k_{0M}}+\frac{\delta L_2}{k_{0A}}-\left(\frac{L_{10}}{k_{0M}^2}\delta k_M+\frac{L_{20}}{k_{0A}^2}\delta k_A\right) \tag{21}$$

(perturbational form of equation 4)

$$\begin{aligned}\delta M&=\tfrac{1}{2}\left(1-\frac{2m\omega_0}{\hbar Q_0^2}\right)q_x+\frac{m}{\hbar Q_0}\delta\omega\\ \delta A&=\tfrac{1}{2}\left(1+\frac{2m\omega_0}{\hbar Q_0^2}\right)q_x-\frac{m}{\hbar Q_0}\delta\omega\\ \alpha&=\frac{q_y}{Q_0}\end{aligned} \tag{22}$$

Table 1. *Coefficients*

$$N = k_{0M}\frac{L_{20}}{k_{0A}} + k_{0A}\frac{L_{10}}{k_{0M}}$$

i	B_{i1}	B_{i2}	B_{i3}
q_x	$\frac{1}{2\alpha_1 k_{0M}}\left\{\frac{L_{20}}{k_{0A}^2 N}\left[M_0\left(1-\frac{2m\omega_0}{\hbar Q_0^2}\right) - A_0\left(1+\frac{2m\omega_0}{\hbar Q_0^2}\right)\right](-2\tan\theta+\cot\varrho) - \frac{\left(1-\frac{2m\omega_0}{\hbar Q_0^2}\right)}{\sin\varrho}\right\}$	$\frac{1}{2\beta_M k_{0M}}\left\{\frac{L_{20}}{k_{0A}^2 N}\left[M_0\left(1-\frac{2m\omega_0}{\hbar Q_0^2}\right) - A_0\left(1+\frac{2m\omega_0}{\hbar Q_0^2}\right)\right](-\tan\theta+\cot\varrho) - \frac{\left(1-\frac{2m\omega_0}{\hbar Q_0^2}\right)}{\sin\varrho}\right\}$	$\frac{L_{10}}{\Delta\mathrm{Ch}\,.\,2k_{0M}}\left\{\frac{L_{20}}{k_{0A}^2 N}\left[M_0\left(1-\frac{2m\omega_0}{\hbar Q_0^2}\right) - A_0\left(1+\frac{2m\omega_0}{\hbar Q_0^2}\right)\right]\cot\varrho - \frac{\left(1-\frac{2m\omega_0}{\hbar Q_0^2}\right)}{\sin\varrho}\right\}$
q_y	$\frac{1}{\alpha_1 Q_0}$	$\frac{1}{\beta_M Q_0}$	$\frac{L_{10}}{\Delta\mathrm{Ch}\,Q_0}$
$\delta\omega$	$\frac{m}{\hbar}\frac{1}{\alpha_1 k_{0M}}\left[\frac{L_{20}}{k_{0A}^2 N}(-2\tan\theta+\cot\varrho) - \frac{1}{\sin\varrho Q_0}\right]$	$\frac{m}{\hbar}\frac{1}{\beta_M k_{0M}}\left[\frac{L_{20}}{k_{0A}^2 N}(-\tan\theta+\cot\varrho) - \frac{1}{\sin\varrho Q_0}\right]$	$\frac{m}{\hbar}\frac{L_{10}}{\Delta\mathrm{Ch}\,k_{0M}}\left[\frac{L_{20}}{k_{0A}^2 N}\cot\varrho - \frac{1}{\sin\varrho Q_0}\right]$
δt	$\frac{-\hbar}{m}\frac{1}{\alpha_1 k_{0M}}\frac{k_{0A}}{N}(-2\tan\theta+\cot\varrho)$	$\frac{-\hbar}{m}\frac{1}{\beta_M k_{0M}}\frac{k_{0A}}{N}(-\tan\theta+\cot\varrho)$	$\frac{-\hbar}{m}\frac{L_{10}\cot\varrho k_{0A}}{\Delta\mathrm{Ch}\,k_{0M}N} - \frac{v_{\mathrm{Ch}}}{\Delta\mathrm{Ch}}$
x	$\frac{1}{\alpha_1 k_{0M}}\frac{\sin\varphi}{N}(-2\tan\theta+\cot\varrho)$	$\frac{1}{\beta_M k_{0M}}\frac{\sin\varphi}{N}(-\tan\theta+\cot\varrho)$	$\frac{L_{10}}{\Delta\mathrm{Ch}\,k_{0M}}\cot\varrho\frac{\sin\varphi}{N} + \frac{1}{\Delta\mathrm{Ch}}$
y	$\frac{1}{\alpha_1 k_{0M}}\frac{1}{N}\left(\cos\varphi - \frac{k_{0A}}{k_{0M}}\right)(-2\tan\theta+\cot\varrho)$	$\frac{1}{\beta_M k_{0M}}\frac{1}{N}\left(\cos\varphi - \frac{k_{0A}}{k_{0M}}\right)(-\tan\theta+\cot\varrho)$	$\frac{L_{10}\cot\varrho}{\Delta\mathrm{Ch}\,k_{0M}}\frac{1}{N}\left(\cos\varphi - \frac{k_{0A}}{k_{0M}}\right)$

(perturbational form of equations 1, 2, 3)

$$\left.\begin{aligned}\gamma_M &= -\frac{\delta M}{k_{0M}\,.\,\sin\varrho} + \frac{\delta k_M}{k_{0M}}\cot\varrho + \alpha\\ \gamma_A &= \frac{\delta A}{k_{0A}\,.\,\sin\lambda} - \frac{\delta k_A}{k_{0A}}\cot\lambda + \alpha\end{aligned}\right\} \tag{23}$$

$$\left.\begin{aligned}U &= L_{10}\gamma_M + y;\\ V &= -L_{20}\gamma_A + x\cos\varphi - y\sin\varphi\end{aligned}\right\}. \tag{24}$$

The overall transmission T of equation (18) can then be written as an exponential of a sum of squares of linear polynomials in q_x, q_y, $\delta\omega$, δt, x, y. The coefficients of these polynomials B_{ij}, i being the variables $i = q_x, q_y, \delta\omega, \delta t, x, y$, j the number of the defining elements, $j = 1 \ldots 7$, are given in Table 1.

The variables δt, x, y are eliminated by integrations in the same way as l, the height of the scattering triangle, in the TAS case. To do this, a 6×6 symmetrical matrix

$$C_{ik} = \sum_{j=1\ldots 7} B_{ij}B_{kj};\quad i,k = q_x, q_y, \delta\omega, \delta t, x, y \tag{25}$$

is formed. The integration over r (r is either δt or x or y) results in a replacement of all elements C_{ik}; $i,k \neq r$ by

$$C'_{ik} = C_{ik} - \frac{C_{ir}C_{kr}}{C_{rr}}. \tag{26}$$

When this procedure has been applied three times, one each for δt, x, y, the resolution coefficients are

$$\begin{aligned}\mathscr{A}_{xx} &= C'''_{qx,qx}\\ \mathscr{A}_{yy} &= C'''_{qy,qy}\\ \mathscr{A}_{\omega\omega} &= C'''_{\delta\omega,\delta\omega}\\ \mathscr{A}_{xy} &= C'''_{qxqy}\\ \mathscr{A}_{x\omega} &= C'''_{qx\delta\omega}\\ \mathscr{A}_{y\omega} &= C'''_{qy\delta\omega}.\end{aligned} \tag{27}$$

We now have to consider the pre-exponential factor, the amplitude of the transmission function density. In the TAS case this amplitude contains a factor $\sqrt{\pi/W_l}$ resulting from the integration of the manifold of $(k_M k_A)$ vector pairs belonging to $\mathbf{Q}_0, \omega_0$, over l. The TAS counter *collects all* the neutrons transmitted. In the present case, there are several 'counters' corresponding to different τ's; assigning the full l-manifold to the 'counter' $(\tau, \tau+\Delta\tau)$ would result in multiple counting of vector pairs $(\mathbf{k}_M, \mathbf{k}_A)$: this is because each pair $(\mathbf{k}_M, \mathbf{k}_A)$ is not only a member of the manifold supported by $\mathbf{Q}_0(\tau)$, $\omega_0(\tau)$ for a specific τ, but also of

B_{ij} *in equation* (25)

B_{i4}	B_{i5}	B_{i6}	B_{i7}
$\frac{L_{10}}{\Delta\mathrm{Ch}\,.\,2k_{0M}}\left\{\frac{L_{20}}{Nk_{0A}^2}\left[M_0\left(1-\frac{2m\omega_0}{\hbar Q_0^2}\right)-A_0\left(1+\frac{2m\omega_0}{\hbar Q_0^2}\right)\right]\cot\varrho-\frac{\left(1-\frac{2m\omega_0}{\hbar Q_0^2}\right)}{\sin\varrho}\right\}$	0	0	$\frac{-L_{20}}{2\Delta Vk_{0A}}\left\{\frac{L_{10}}{k_{0M}^2N}\left[M_0\left(1-\frac{2m\omega_0}{\hbar Q_0^2}\right)-A_0\left(1+\frac{2m\omega_0}{\hbar Q_0^2}\right)\cot\lambda+\frac{\left(1+\frac{2m\omega_0}{\hbar Q_0^2}\right)}{\sin\lambda}\right.\right.$
$\frac{L_{10}}{\Delta\mathrm{Ch}Q_0}$	0	0	$-\frac{L_{20}}{\Delta VQ_0}$
$\frac{m}{\hbar}\frac{L_{10}}{\Delta\mathrm{Ch}k_{0M}}\left[\frac{L_{20}}{k_{0A}^2N}\cot\varrho-\frac{1}{\sin\varrho Q_0}\right]$	0	0	$-\frac{m}{\hbar}\left(-\frac{L_{20}}{\Delta Vk_{0A}}\right)\left[\frac{L_{10}}{k_{0M}^2N}\cot\lambda-\frac{1}{Q_0\sin\lambda}\right]$
$\frac{-\hbar}{m}\frac{L_{10}}{\Delta\mathrm{Ch}k_{0M}}\cot\varrho\frac{k_{0A}}{N}$	0	0	$\frac{-\hbar}{m}\frac{L_{20}}{\Delta Vk_{0A}}\cot\lambda\frac{k_{0M}}{N}$
$\frac{L_{10}}{\Delta\mathrm{Ch}k_{0M}}\cot\varrho\frac{\sin\varphi}{N}+\frac{1}{\Delta\mathrm{Ch}}$	$\frac{1}{\Delta r}$	0	$\frac{L_{20}}{\Delta Vk_{0A}}\cot\lambda\frac{k_{0M}}{k_{0A}N}+\frac{\cos\varphi}{\Delta V}$
$\frac{L_{10}\cot\varrho}{\Delta\mathrm{Ch}k_{0M}}\frac{1}{N}\left(\cos\varphi-\frac{k_{0A}}{k_{0M}}\right)$	0	$\frac{1}{\Delta r}$	$\frac{L_{20}}{\Delta Vk_{0A}}\cot\lambda\frac{1}{N}\left(\cos\varphi\frac{k_{0M}}{k_{0A}}-1\right)-\frac{\sin\varphi}{\Delta V}$

the manifold supported by $\mathbf{Q}_0(\tau')$, $\omega_0(\tau')$, with different q_x, q_y, $\delta\omega$ in the two families. To avoid this multiple counting, one has to assign only a small piece δl of l, around l_0, to the counter $(\tau, \tau+\delta\tau)$, where δl and $\delta\tau$ are related by the change of the *nominal* triangle $\mathbf{k}_{0M}(\tau)$, $\mathbf{k}_{0A}(\tau)$, $\mathbf{Q}_0(\tau)$ with τ, as shown in Fig. 3:

$$\delta l=\delta k_{0A}\sin\lambda\cos\varrho\frac{k_{0M}}{Q_0} \tag{28}$$

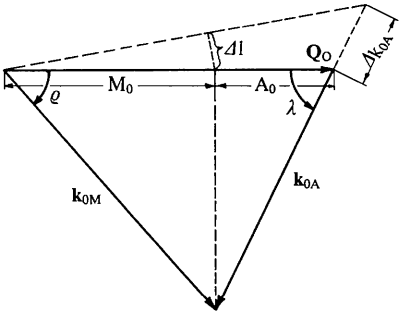

Fig. 3. The relation between $\Delta\mathbf{k}_{0A}$ and Δl leading, through equations (28), (29) to $\mathrm{d}l/\mathrm{d}\tau$ of equation (30).

and, from equation (8)

$$\delta\tau=-\frac{m}{\hbar}\frac{L_{20}}{k_{0A}^2(\tau)}\delta k_{0A} \tag{29}$$

are combined, with the result

$$\left|\frac{\delta l}{\delta\tau}\right|=\frac{\sin\lambda\cos\varrho\,k_{0M}}{Q_0}\frac{\hbar}{m}\frac{k_{0A}^2(\tau)}{L_{20}}, \tag{30}$$

which has to be inserted instead of the $\sqrt{\pi/W_l}$, the TAS factor. Another intensity factor is DC, the duty cycle, which is due to the fact that with a continuous neutron source only this proportion of all neutrons complying with the **k**-space restrictions accounted for in our calculations, pass the spectrometer.

Finally, multiplying by $\Delta\tau$ (the channel width) and using the pre-exponential factor

$$\frac{P_M(k_{0M})\epsilon(k_{0A})}{2k_{0M}^3Q_0}V(q_z)\sqrt{\frac{\pi}{W_z}}$$

(Quittner, 1971, 1972), where $P_M(k_{0M})$ is the crystal top reflectivity, $\epsilon(k_{0A})$ the counter efficiency, $V(q_z)$ is the vertical resolution function of the Appendix equation (A4) and $\sqrt{\pi/W_z}$, the factor in Appendix equation (A5), the transmission function of a channel $\Delta\tau$ is

$$\mathscr{F}(Q,\omega;\Delta\tau)=\frac{P_M(k_{0M})\epsilon(k_{0A})}{2k_{0M}^3Q_0}V(q_z)\sqrt{\frac{\pi}{W_z}}$$
$$\times\frac{1}{(\Delta r)^2\sqrt{W_xW_y}}\frac{\hbar}{m}\frac{\sin\lambda\cos\varrho k_{0M}}{Q_0}\frac{k_{0A}^2}{L_{20}}\mathrm{DC}$$
$$\times\exp-[\mathscr{A}_{xx}q_x^2+\mathscr{A}_{yy}q_y^2+\mathscr{A}_{\omega\omega}\delta_\omega^2$$
$$+2\mathscr{A}_{xy}q_xq_y+2\mathscr{A}_{x\omega}q_x\delta\omega+2\mathscr{A}_{y\omega}q_y\delta\omega]\Delta\tau.^*\quad(31)$$

The counting rate into the channel is (Quittner, 1971)

$$\mathrm{C.R.}(\Delta\tau)=\frac{\phi_0(k_{0M})}{4\pi}\int\mathscr{F}(\mathbf{Q},\omega;\Delta\tau)S(\mathbf{Q},\omega)\mathrm{d}\mathbf{Q}\mathrm{d}\omega.\quad(32)$$

It should be noted that except for P_M, k_{0M}, Δr, L_{20} and DC all pre-exponential factors in (28) depend on $k_{0A}(\tau)$. This dependence, together with the 'trivial' factors of Quittner (1971), § 6, influences the relation between the time-of-flight spectrum and the sample's $S(\mathbf{Q},\omega)$ along an appropriate path in $(\mathbf{Q},\omega)$. This is a much-debated problem with time-of-flight spectrometers and has been approached in the past without considering the transmission function.

The calculation assumed the 'N' arrangement of Fig. 2. When the sign of the scattering angle is changed (into the 'U' arrangement') the sign of $\sin\varrho$ and $\sin\lambda$ must be changed. Similarly, when the chopper rotates in a sense contrary to that of Fig. 2, the sign of v_{Ch} must be changed.

Spectrometers different in detail from the present model can be treated in the same way by changing $T_1 \ldots T_7$ and modifying the real space equations (23, 24), whereas equations (19) to (22) remain valid.

Another interesting number is the time-of-flight width of the vanadium peak. The cross section of vanadium is constant over $\mathbf{Q}$ and selects zero energy transfers. It can be calculated by first integrating the coefficient scheme $C'''_{i,k}$ over q_x,q_y by the same reduction formula (25), r being this time q_x and q_y. This results in an energy width

$$\omega_{1/2}=\sqrt{\ln 2}\,.\,(C''''''_{\delta\omega\delta\omega})^{-1/2}.\quad(33)$$

This combined with the relation between $\omega_0(\tau)$ of the supporting point and τ (equations 5, 8) results in

$$\mathrm{FWHM}(\tau)=2\left(\frac{m}{\hbar}\right)^2\frac{L_{20}}{k_{0A}^3}\omega_{1/2}.\quad(34)$$

4. Numerical example and problems of accuracy

The following input data:

$\omega_0=0$ (elastic channel)

$k_{0M}=k_{0A}=1{\cdot}285\times10^8\ \mathrm{cm}^{-1}$; $\varphi=81{\cdot}9°$

$\varrho=\lambda=49{\cdot}05°$; $\theta=90°$; $\alpha_1=0{\cdot}6°$

$\beta_M=0{\cdot}5°$, $\Delta\mathrm{Ch}=\Delta r=\Delta V=1{\cdot}2$ cm

$v_{\mathrm{Ch}}=13572\ \mathrm{cm\ s}^{-1}$; $L_{10}=30$ cm; $L_{20}=130$ cm

result in

$$\mathscr{A}_{xx}=6562\times10^{-16}\ \mathrm{cm}^2$$
$$\mathscr{A}_{yy}=4583\times10^{-16}\ \mathrm{cm}^2$$
$$\mathscr{A}_{\omega\omega}=14667\times10^{-26}\ \mathrm{s}^{-2}$$
$$\mathscr{A}_{xy}=-3399\times10^{-16}\ \mathrm{cm}^2$$
$$\mathscr{A}_{x\omega}=8723\times10^{-21}\ \mathrm{cm\ s}^{-1}$$
$$\mathscr{A}_{y\omega}=7366\times10^{-21}\ \mathrm{cm\ s}^{-1}$$

and

$$\mathrm{FWHM}(\tau)=0{\cdot}18\times10^{-3}\ \mathrm{s}.$$

A serious practical problem is the error propagation by the formula (25), already for the resolution coefficients, where it has to be applied three times; and even more for the energy width (equation 34) where it has to be applied five times.

The inaccuracies arise when the product of the off-axis (mixed) terms $C_{ir}C_{kr}$ in equation (26) is not small compared with the product $C_{ik}C_{rr}$ of the axis terms, *i.e.* when the six-dimensional ellipsoid $\exp\left[-\sum_{ik}C_{ik}x_ix_k\right]$ is strongly elongated along directions other than the axes q_x, q_y, $\delta\omega$, δt, x, y. Strong cancellations and error magnifications are the consequence. This is due to the subtractions inherent in formula (25). In our numerical example the original coefficient $C_{\delta\omega\delta\omega}$ is a factor 2500 larger than the result $C''''''_{\delta\omega\delta\omega}$ used for $\omega_{1/2}$. The numbers C_{ik}, C'_{ik} *etc.* must be kept at about nine figures to obtain an accuracy of 5–10% only, in $\omega_{1/2}$. In principle these error propagation properties depend on the choice of axes in the six-dimensional space of q_x, q_y, $\delta\omega$ and the three other variables, and in fact, things would be even worse had we, for example, chosen l, the height of the scattering triangle instead of δt, as would be natural to keep the analogy with the TAS case.

It is not within the scope of the present paper to offer other possible more sophisticated schemes of calculation avoiding these numerical problems. It should be emphasized however that this problem exists, and can be solved by using, starting from the B_{ij}, accuracies (of the order of 10 digits or more) far higher than those one would choose from consideration of the physical accuracies of the input numbers.

The author is indebted to Dr G. Ernst for useful discussions on topics of § 4.

APPENDIX

Definitions of some factors occuring in equation (31)

$$W_x=C'_{xx}\quad(A1)$$

$$W_y=C''_{yy}\quad(A2)$$

$$S_{VM}=\left(\frac{1}{\alpha_{1V}^2+4\sin^2\theta\beta_{MV}^2}+\frac{1}{\alpha_{2V}^2}\right)^{-1/2}\quad(A3)$$

* For definitions of W_x, W_y see Appendix.

$$V(q_z)=\exp-\left(\frac{q_z^2}{k_{0M}^2S_{VM}^2+k_{0A}^2\alpha_{3V}^2}\right) \quad \text{(A4)}$$

$$W_z=\left(1+\frac{4\sin^2\theta\beta_V^2}{\alpha_{1V}^2}\right)\left(\frac{1}{k_{0M}^2S_{VM}^2}+\frac{1}{k_{0A}^2\alpha_{3V}^2}\right) \quad \text{(A5)}$$

References

BAUER, G., SEITZ, E. & JUST, W. (1975). *J. Appl. Cryst.* **8**, 162–175.

COOPER, M. J. & NATHANS, R. (1967). *Acta Cryst.* **23**, 357–367.

KLEB, R., OSTROWSKI, G. E., PRICE, D. L. & ROWE, J. M. (1973). *Nucl. Instrum. Meth.* **106**, 221–230.

KOMURA, S. & COOPER, M. J. (1970). *Jap. J. Appl. Phys.* **9**, 866–874.

NIELSEN, M. & BJERRUM-MØLLER, H. (1969). *Acta Cryst.* A**25**, 547–550.

QUITTNER, G. (1971). *Acta Cryst.* A**27**, 605–612; *erratum* (1972). A**28**, 464.

SAMUELSEN, E. J. (1971). *Structural Phase Transitions and Soft Modes*, pp. 189–215. *Proc. NATO Adv. Study Inst. Geilo.* Oslo: Universitetsforlaget.

STEINSVOLL, O. (1973). *Nucl. Instrum. Meth.* **106**, 453–459.

Acta Cryst. (1977). A**33**, 307–310

Relations entre la Symétrie Moléculaire et le Groupe Spatial de Cristallisation: Cas des Molécules Possedant un Axe Binaire

PAR MARIE-CLAIRE BRIANSO

Laboratoire de Minéralogie–Cristallographie associé au CNRS, Université Pierre et Marie Curie, 4 place Jussieu, 75230 Paris Cédex 05, France

(*Reçu le 24 juin 1976, accepté le 29 septembre 1976*)

Among the chiral molecules which crystallize as conglomerates, 25% are twofold molecules. Some simple packing hypotheses bounded by molecular symmetry permit one to select, with Belov's plane groups, some probable space groups. Only the cases of the primitive lattice and monoclinic and orthorhombic systems are treated.

Introduction

Une étude systématique (effectuée sur 750 cas) des possibilitiés de dédoublement spontané de composés à molécules chirales montre que seulement 10 à 12% cristallisent sous forme de conglomérat; parmi ces derniers composés, 25% sont constitués de molécules présentant une symétrie binaire (Collet, Brienne & Jacques, 1972). Il semble donc que l'existence d'un axe binaire pour la molécule augmente les chances de dédoublement spontané.

Certains auteurs, dont Pedone & Benedetti (1972), se sont intéressés aux relations structurales entre les solides racémiques et énantiomères: parfois un plan, plus souvent une colonne moléculaire, sont communs aux deux empilements structuraux.

Nous avons étudié plus particulièrement le cas de composés chiraux, dont la molécule possède *un axe binaire*, et essayé d'envisager une systématique reliant divers dérivés *trans*-1,2 de l'acénaphtène.

Nous avons remarqué, pour chaque cristal étudié, les éléments structuraux suivants: existence de colonnes homochirales, parallèles à un vecteur période de la maille élémentaire; empilement mettant en évidence un axe binaire hélicoïdal perpendiculaire à l'axe de cette colonne.

Une explication s'appuyant sur des considérations électrostatiques peut être proposée. (1) Associons un dipôle à chaque molécule. La construction d'une colonne de molécules homochirales nécessite de placer les molécules de telle sorte que leur dipôle s'oriente selon une position d'énergie minimale, c'est-à-dire telle que les charges se compensent deux à deux. Lorsque la molécule possède un axe de symétrie, le moment dipôlaire est un vecteur parallèle à l'axe; l'empilement moléculaire se fera de préférence parallèlement à cet axe; la période peut alors être associée à un vecteur cristallographique. (2) La présence d'un axe binaire hélicoïdal est très fréquente pour les composés moléculaires. Ceci est signalé dans les études statistiques effectuées par Zorkii & Bel'skii (1971) ainsi que dans les résultats de la théorie de l'empilement compact développée par Kitaigorodskii (1962).

Les avantages électrostatiques sont immédiats: un axe binaire hélicoïdal perpendiculaire à l'axe des charges du dipôle a le privilège de les placer de telle sorte que: les charges locales se compensent par leur voisinage immédiat; les moments dipôlaires sont opposés (leurs effets s'annulent donc globalement).

Nous nous proposons de chercher les groupes spatiaux compatibles avec les conditions suivantes: réseau de Bravais de type P avec $Z=2$ ou 4; type moléculaire possédant un axe binaire vrai; empilement moléculaire linéaire selon un axe qui coïncide avec un vecteur période du réseau cristallin; existence, dans la maille élémentaire, d'un axe binaire hélicoïdal perpendiculaire à l'axe de la molécule.

Nous nous limiterons aux symétries monoclinique